BULLETIN OF THE POLISH ACADEMY OF SCIENCES
TECHNICAL SCIENCES
Vol. 57, No. 1, 2009

Electrostatic deposition of nanothin films on metal substrate[§]

A. JAWOREK*, A.T. SOBCZYK, A. KRUPA, M. LACKOWSKI, and T. CZECH

The Szewalski Institute of Fluid-Flow Machinery, Polish Academy of Sciences, 14 Fiszera St., 80-952 Gdańsk, Poland

Abstract. Thin solid film has been deposited by electrohydrodynamic spraying (electrospraying) onto a metal substrate. Electrospraying is a low-energy physical process in which tangential stress exerted by electric field on the surface of a liquid flowing form a capillary nozzle causes jet elongation, and the Coulomb repulsive forces disintegrate of this jet into fine droplets. By this method TiO_2, ZnO, MgO, or Al_2O_3 particles of size from 20 to 100 nm electrosprayed from a colloidal suspension were deposited onto a stainless steel substrate. The advantage that electrospray has over other methods for thin solid film production is that the growth rate of the layer is relatively high, the process can be carried out in an ambient atmosphere, in air or other gas, and at low temperature, without the need for a complex reactor and vacuum systems.

Key words: electrospray deposition, metal-oxide layer.

1. Introduction

Electrohydrodynamic spraying (electrospraying) has been utilized as a means for the deposition of thin solid films of thickness 100–200 nm on a metal substrate. Electrospraying is a low-energy physical process in which tangential stress is exerted by electric field on the surface of a liquid flowing form a capillary nozzle. This stress causes jet elongation, and next, the repulsive Coulomb forces disintegrate the jet into fine droplets. To this goal, the nozzle has to be connected to a high electric potential. A counter electrode, which can be a substrate or an extractor, has to be grounded.

Various forms of jet instabilities, known as spraying modes, have been observed and reported in the literature [1–11], however in practice, only some of these modes can be useful in practice. For the purpose of thin film deposition only cone-jet and multijet modes are of practical importance. This is because only in these modes, sufficiently fine droplets, of micron size, and of narrow size distribution can be obtained. Small droplets of a solution or colloidal suspension can provide films of thickness smaller than 1000 nm, depending on the solute concentration or size of suspended particles. The selection of proper materials to be deposited allows production of functional layers of required physical, thermal, or mechanical properties. Electrospray method was also tested by many authors for the production of nanocomposite materials or for direct writing (patterning), a technique which is capable of producing structures of width finer than 10 μm [12–16]. An advantage of electrospray-made composite products is that the composition can be changed on demand during the production process. Electrospray composites were formed from, for example, alumina-titania [17] or aluminum-rutile [18] components.

The purpose of this paper is to demonstrate the electrospray method as a means for thin solid film deposition on a metal substrate for thermal and corrosion protection of a material. By this method TiO_2, ZnO, MgO, or Al_2O_3 particles of size from 20 to 100 nm were deposited. The advantage that electrospray has over other methods for thin solid film production is that the growth rate of the layer is relatively high. The process can be carried out in an ambient atmosphere, in air or other gas, and at low temperature, without the need for a complex reactor and vacuum systems. The deposited material is not damaged in this process that is important in the case of biological substances. The electrospray can produce highly pure materials with structural control at the nanometer scale. The crystallinity, texture, film thickness, and deposition rate can be controlled by adjusting voltage, flow rate, and the substrate temperature [19, 20]. Microscope inspections confirmed that electrospray deposited layer is even, without micro-fissures and structural dislocations. The electrospray is a very efficient process because at least 80–90% of the solution can be deposited onto the substrate. Compared to conventional nozzles, electrospray nozzle can be an order of magnitude larger than the produced droplet size that prevents nozzle clogging.

2. Experimental

The electrospray system consisted of a stainless-steel capillary nozzle and a heated stainless steel table of diameter of 120 mm. The distance between the nozzle tip and the table was 15 or 25 mm. The substrate was a stainless steel rectangular plate 500 μm thick and of the dimensions of 25×30 mm. In order to facilitate solvent evaporation, the substrate was electrically heated by an electric heater placed beneath the table. The temperature of the substrate was about 70–90°C. At the level of the needle tip a grounded extractor electrode, in the form of ring of inner diameter of 30 mm, was mounted in order to improve meniscus and droplet formation in the electric field, and wider distribution of the spray plume over the substrate. The dimensions of the capillary and electro-

[§]Presented at 1st National Conference of Nano and Micro Mechanics (KKNM08), Krasiczyn, July 2008.

*e-mail: jaworek@imp.gda.pl

spraying conditions are specified in the caption to each figure presenting the experimental results.

The nozzle was connected to a high voltage ac/dc generator PM04015 TREK switched to positive polarity, while the plate and extractor electrodes were grounded. The spray plume was recorded using CCD camera PANASONIC NV-GS 400.

The liquid was supplied through a polyethylene pipe 0.8 mm inner diameter, from a syringe pump AP22 (Ascor – Poland) mounted above the nozzle. Methanol used as a solvent in these experiments was purchased from POCH Gliwice (Poland). MgO particles of 40.3 g/mol (99% metals basis) and size 100 nm, TiO_2 particles of molecular weight of 79.9 g/mol (99.9% metals basis) and mean diameter 29 nm, ZnO particles of molecular weight of 81.37 g/mol (>99% metals basis) and mean diameter 71 nm, and Al_2O_3 particles of molecular weight 101.96 g/mol (99.6% purity) and mean diameter 30 nm were purchased from Alfa Aesar.

The suspensions were prepared by stirring the commercial nanopowder in a mixture of different fraction of ethylene glycol and methanol in a glass vessel for 24 h. A small amount of Dynasylan®Memo purchased from Degussa was added as suspension dispersant. Next the suspension was loaded to a syringe and mounted in the syringe pump.

A schematic illustrating the principle of electrospray thin solid layer deposition is shown in Fig. 1. The substrate was heated during electrospraying process (Fig. 1, left), and after the voltage was switched-off, the heating was continued to complete solvent evaporation (Fig. 1, right). The suspensions were electrosprayed for a time of 30–60 min. The flow rate of the suspensions was set to 1 or 1.5 ml/h. The detailed data of the experimental conditions are specified in captions to each figure. The produced structures were examined under a scanning electron microscope EVO-40 (Zeiss).

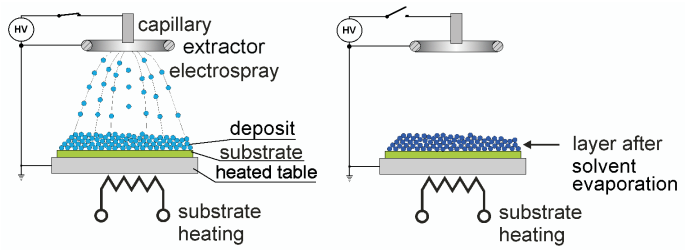

Fig. 1. Schematic of electrospray system for thin layer deposition from a suspension

3. Results

Electrospray deposition was applied for thin layer production from a suspension of a material to be deposited. The spray system used in the experiments operated in the cone-jet mode or multi-jet mode. The multi-jet mode made it possible to obtain simultaneously a large number of emission cones from a single capillary, and the droplets can be smaller than from a single cone. The electrospray droplets were targeted onto a metal substrate to form a tight solid layer on it after solvent evaporation. Evaporation can be speeded-up by heating the substrate during the deposition process or after it.

An ac/dc supply voltage was used in our experiments to the electrospray nozzle. It was noticed that sine-wave ac voltage superimposed on dc bias stabilizes the cone-jet mode of spraying and the spray plume. The frequency was 314 Hz in this experimental condition, and it was tuned to the middle of frequency range of the stabilizing effect. The dc bias was in the range from 5.7 to 6.3 kV, and ac voltage was in the range from 1.5 to 4 kV_{p-p}. The voltages and ac frequency, and flow rate were chosen experimentally for each electrosprayed material and electrode distance separately via observation of the electrospray mode and spray plume distribution. The spraying conditions were set to obtain a stable electrospraying mode. Figure 2 shows an electrospraying system with a multi-jet aerosol plume.

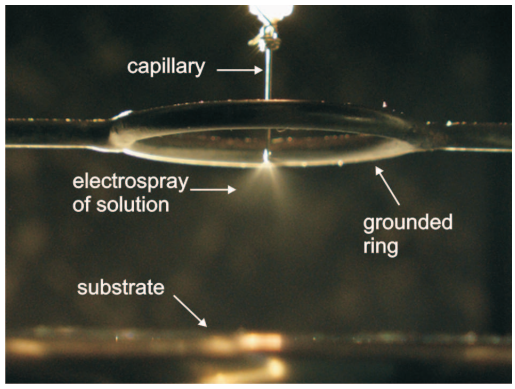

Fig. 2. Photograph of electrospray system

As a result of electrospraying of suspension of a material to be deposited, homogeneous metal-oxides films were obtained. The films were composed of small agglomerates, smaller than a couple of microns, built from the particles of dry powder used for preparing the suspension. The agglomerates were formed during the solvent evaporation from the droplet on its flight towards the substrate. The lower is the concentration of the suspension the smaller are the agglomerates.

SEM images of the layers deposited on a stainless steel plate are shown in Figs. 3–12. The voltage to the capillary and other important parameters are specified in the caption to each figure.

Figures. 3–6 present MgO deposit on a stainless steel substrate at various magnifications and for two regions of the deposit. Figures 3 and 4 show a region under the capillary nozzle, and Figs. 5 and 6 at periphery of the deposit. On this example it is shown that the layer is different depending on the region on the deposit Close-up view shows that layer at the edge is grainy with the grain size of about 1–2 μm. The layer under nozzle is composed of large particle agglomerates, whereas at the edge, the clusters are smaller and the layer is more uniform. This can be explained by different droplets deposition. Close to the capillary nozzle axis, large droplets of higher inertia are deposited. Smaller droplets, of lower mass are easily deflected by the repelling electric field, and are landing near the edge of the plate. Smaller crystallites were therefore formed at this region.

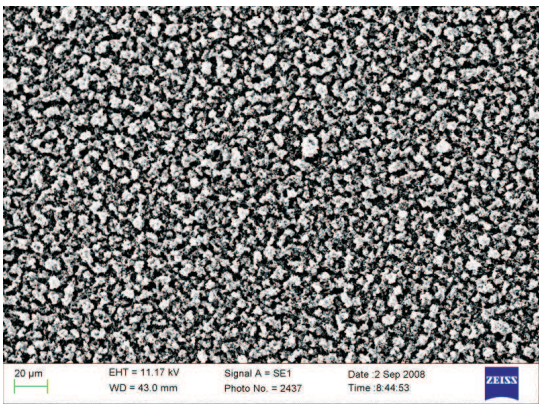

Fig. 3. SEM image of MgO particle layer deposited by electrospraying on a stainless steel substrate at the center of plate under needle electrode (MgO suspension in methanol, weight fraction = 0.06, voltage = 5.7 $kV_{DC} + 3.8$ kV_{AC}, capillary 450 μm o.d., 250 μm i.d., deposition time 40 min, distance between the capillary nozzle and substrate plate 15 mm, flow rate = 1.5 ml/h)

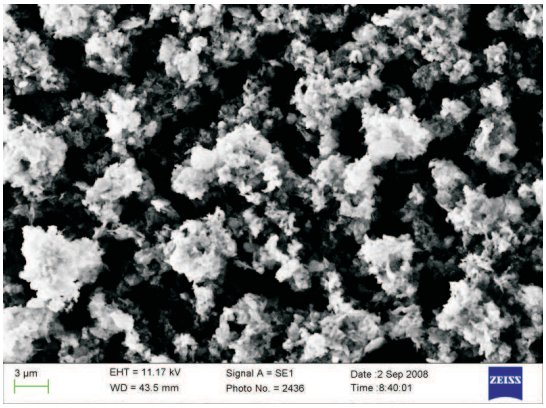

Fig. 4. SEM image of MgO particle layer deposited by electrospraying on a stainless steel substrate at the center of plate under needle electrode (MgO suspension in methanol, weight fraction = 0.06, voltage= 5.7 $kV_{DC} + 3.8$ kV_{AC}, capillary 450 μm o.d., 250 μm i.d., deposition time 40 min, distance between the capillary nozzle and substrate plate 15 mm, flow rate = 1.5 ml/h)

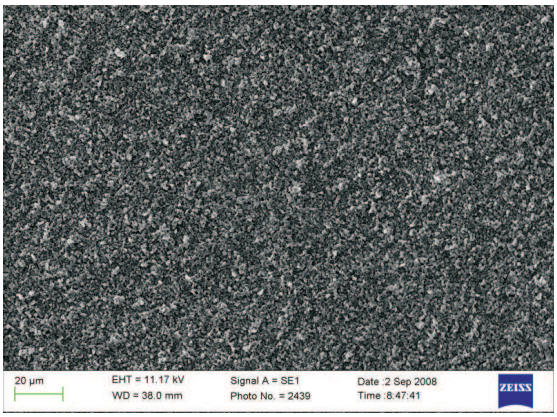

Fig. 5. SEM image of MgO particle layer deposited by electrospraying on a stainless steel substrate at the edge of deposit (MgO suspension in methanol, weight fraction = 0.06, voltage = 5.7 $kV_{DC} + 3.8$ kV_{AC}, capillary 450 μm o.d., 250 μm i.d., deposition time 40 min, distance between the capillary nozzle and substrate plate 15 mm, flow rate = 1.5 ml/h)

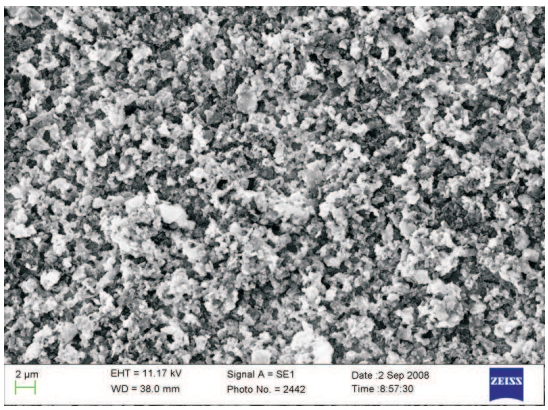

Fig. 6. SEM image of MgO particle layer deposited by electrospraying on a stainless steel substrate at the edge of deposit (MgO suspension in methanol, weight fraction = 0.06, voltage= 5.7 $kV_{DC} + 3.8$ kV_{AC}, capillary 450 μm o.d., 250 μm i.d., deposition time 40 min, distance between the capillary nozzle and substrate plate 15 mm, flow rate = 1.5 ml/h)

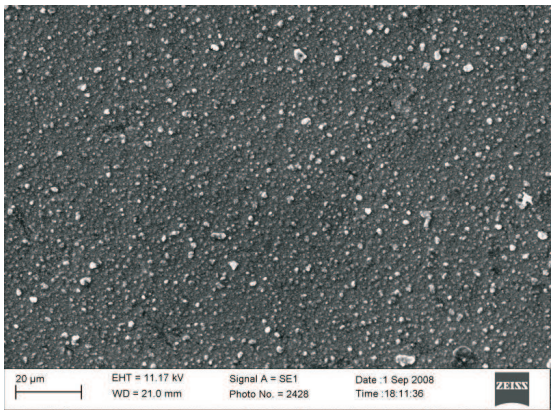

Fig. 7. SEM image of TiO_2 particle layer deposited by electrospraying on a stainless steel substrate (TiO_2 suspension in methanol, weight fraction = 0.06, voltage = 6.3 $kV_{DC} + 4$ kV_{AC}, capillary 450 μm o.d., 250 μm i.d., deposition time 60 min, distance between the capillary nozzle and substrate plate 15 mm, flow rate = 1 ml/h)

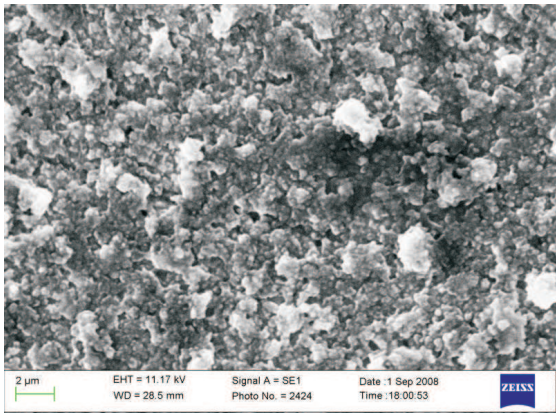

Fig. 8. SEM image of TiO_2 particle layer deposited by electrospraying on a stainless steel substrate (TiO_2 suspension in methanol, weight fraction = 0.06, voltage = 6.3 $kV_{DC} + 4$ kV_{AC}, capillary 450 μm o.d., 250 μm i.d., deposition time 60 min, distance between the capillary nozzle and substrate plate 15 mm, flow rate = 1 ml/h)

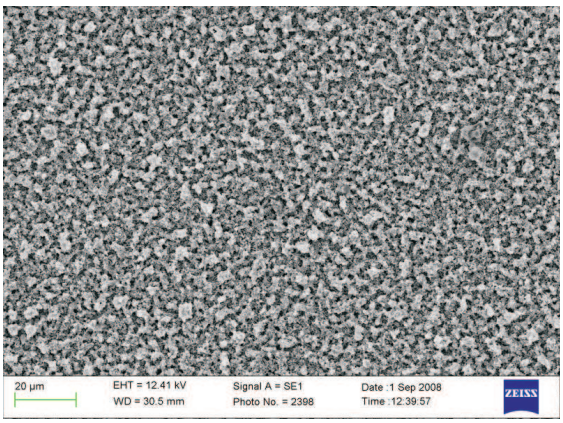

Fig. 9. SEM image of ZnO particle layer deposited by electrospraying on a stainless steel substrate (ZnO suspension in methanol, weight fraction = 0.06, voltage = 6 $kV_{DC} + 2$ kV_{AC}, capillary 450 μm o.d., 250 μm i.d., deposition time 60 min, distance between the capillary nozzle and substrate plate 15 mm, flow rate = 3 ml/h)

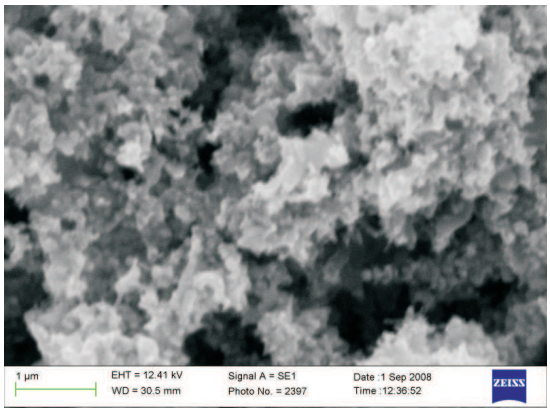

Fig. 10. SEM image of ZnO particle layer deposited by electrospraying on a stainless steel substrate (ZnO suspension in methanol, weight fraction = 0.06, voltage = 6 $kV_{DC} + 2$ kV_{AC}, capillary 450 μm o.d., 250 μm i.d., deposition time 60 min, distance between the capillary nozzle and substrate plate 15 mm, flow rate = 3 ml/h)

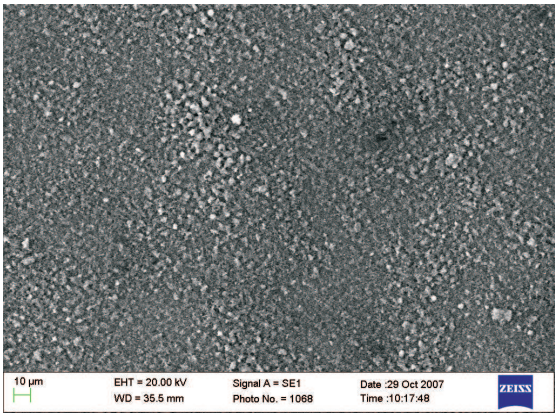

Fig. 11. SEM image of Al_2O_3 α particle layer deposited by electrospraying on a stainless steel substrate (Al_2O_3 α suspension in methanol, weight fraction = 0.06, voltage = 17 $kV_{DC} + 2.5$ kV_{AC}, capillary 450 μm o.d., 250 μm i.d., deposition time about 10 min, volume of sprayed solution 2 ml, distance between the capillary nozzle and substrate plate 25 mm)

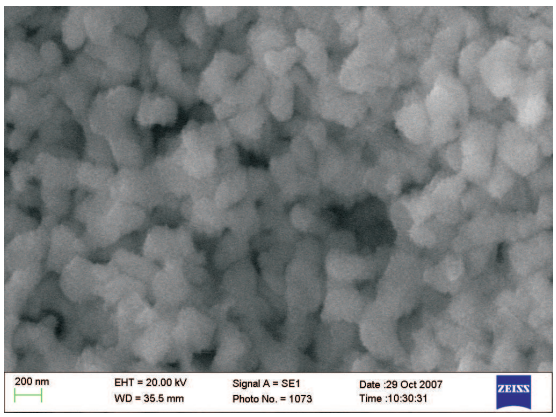

Fig. 12. SEM image of Al_2O_3 α particle layer deposited by electrospraying on a stainless steel substrate (Al_2O_3 α suspension in methanol, weight fraction = 0.06, voltage = 17 $kV_{DC} + 2$ kV_{AC}, capillary 450 μm o.d., 250 μm i.d., deposition time about 10 min, volume of sprayed solution 2 ml, distance between the capillary nozzle and substrate plate 25 mm)

Figures 7 and 8 show the layers of TiO_2 deposited onto the stainless steel substrate. The voltage supplying the capillary was 6.3 $kV_{DC} + 4$ kV_{AC}. The layer consists of flake-like clusters and separate nanoparticles. Few larger grains (about 3 μm in size) can also be observed (Fig. 7).

In Figs. 9 and 10 fragments of the layer of ZnO nanoparticles are shown. The layer of ZnO consists of irregular crystal flakes and has many cracks. The particles of the size 100-200 nm forming the layer can be readily noticed (Fig. 10).

$\alpha - Al_2O_3$ deposit on the stainless steel substrate for various magnifications is presented in Figs. 11 and 12. The particles form a tight layer of particles without visible agglomerates. Larger particles (1–2 μm in diameter in Fig. 11) are probably an effect of coagulation of the smaller ones.

4. Discussion

Thin solid films, thinner than a couple of microns, can be used in manufacturing micro- and nano- electromechanical systems (MEMS or NEMS), in microelectronic devices as semiconducting, insulating or conducting layers, or to improve surface properties of mechanical elements. There are several conventional methods available for thin film deposition on a substrate:

1. Casting of a solution or colloidal suspension on a substrate, followed by solvent evaporation,
2. Cathode spraying, applicable to metal layer preparation,
3. Condensation of vapors of a material on the substrate,
4. Laser ablation for material evaporation,
5. Chemical vapor deposition and plasma assisted/enhanced chemical vapor deposition,
6. Physical vapor deposition,
7. Electroplating, applicable only to metal film formation.

As reported in the literature, in specific cases, the electrosprayed layer exhibited better properties than those obtained by other methods, for example chemical vapor deposition or physical vapor deposition.

Although at the current state of knowledge it is not possible to predict which method of nanothin layer deposition could be commercialized as the most effective, researchers from various laboratories are testing all of the possible solutions. Recently, many researchers have tested the electrospray technique as a means for functional layer deposition from aerosol phase. Usually, the material to be deposited is sprayed directly onto the substrate but the layer can also be formed from a precursor, i.e., a compound, which is decomposed at high temperature or converted to another substance in chemical reactions with other compound sprayed simultaneously or delivered in the gaseous phase. Usually, metal nitrates or acetates dissolved in water, methanol, ethanol, or their mixtures are electrosprayed as precursors for metal-oxide layer production. This process is more complex and needs more precautions than deposition a layer from a suspension. Therefore, for layers thicker than 100 nm, electrospray deposition of a material from a suspension can be used. It is a simpler process, which does not require special chemical reactions and precautions due to possible toxicity of the electrosprayed compounds. This process also seems to be cheaper in the mass production. The layer deposition from a suspension, however, frequently requires sintering the material in order to stabilize the layer. A literature review of thin film deposited from electrosprayed suspensions is presented in Table 1.

The current and potential commercial applications of functional layers produced from a suspension via electrospraying are as follows:

1. Dielectric layers for microelectronic devices formed from alumina (Al_2O_3) or silica (SiO_2) [13, 21–32]. The same metal oxides were also used as corrosion and thermal protection layers.
2. ZrO_2:Y_2O_3 (Yttria-Stabilized-Zirconia – YSZ). nanoparticles have found application as solid electrolyte [33], while platinum particles as electrodes [34], in fuel cells.
3. Gold or silver nanoparticles were deposited as nanowires for nanoelectronic applications [13, 35–38].
4. Nickel nanoparticles were deposited as seeds for amorphous silicon growth [39].
5. Solid lubricating films of molybdenite (MoS_2) were obtained by electrospraying of MoS_2 suspension [40, 41].
6. Composite ceramics from alumina-zirconia [42] or zirconia-silicon carbide [29] were also produced via electrospraying of suspensions.
7. Superhydrophobic coating for the production of self-cleaning materials was electrospray – deposited from fine PTFE particles of the size 50–500 nm suspended in water [43, 44].
8. PZT (lead zirconate titanate) microcoatings are or potentially can be applied as piezoelectric micro-sensors, ferroelectric capacitors, piezoelectric micro actuators, or non-volatile random access memory due to excellent piezoelectric, ferroelectric and dielectric properties of this material. The PZT layers were, for example, produced by Lu et al. [45], Wang and Derby [46], and recently by Sun et al. [47].
9. Hydroxyapatite nanoparticles or relics deposited on various substrates were investigated with the goal for the formation of implants for bone repair, or orthopaedic and dental implants manufacturing [15, 16, 48–53], or for the creation of micro- and nano-scale surface morphology for a favorable cell response [49].

Review of the production of thin layers via electrospraying of appropriate precursors or from various suspensions can be found in [19, 20].

Our results with metal oxide nanoparticles confirmed earlier reports that the films produced by electrospraying can be homogeneous and composed of small agglomerates built of nanoparticles forming the suspension. The quality of thin film formed on a substrate strongly depends on the size of particles or droplets forming the layer, and their monodispersity. Even layers, of uniform thickness are obtained when the droplets are uniformly dispersed over the substrate. Smaller particles, of narrow size distribution are required in order to reduce the number and size of voids, flaws and cracks in the film. The electrospray allows generating fine droplets in micro- and submicron size range, with narrow size distribution. Electrostatic forces disperse the droplets homogeneously in the space between the nozzle and the substrate. The film thickness, its texture, and deposition rate can be controlled by varying the voltage, flow rate, concentration of the material to be deposited, and the substrate temperature.

Regardless of promising results presented in this and other papers, several problems have to be solved. The most important is stability of the electrospraying mode. Small changes in liquid properties (due, for example, to temperature variation) can switch the spraying mode from that generating submicron droplets to another one, sputtering the liquid. The layer uniformity depends also on the deposited material, and the spraying conditions should be set for a specific material separately. We also noticed that adding of a surfactant can improve the layer quality, but for some materials can cause larger agglomerates formation.

A novelty in our experiments is using ac/dc excitation of the electrospray nozzle in order to thin layer deposition. It was noticed that sine-wave ac voltage of frequency 314 Hz superimposed on dc bias could stabilize the cone-jet mode of spraying and the spray plume. Excitation at this frequency is certainly not a synchronous droplet generation, which ought to be at least tens of kHz.

Table 1
Submicron films produced from suspensions deposited by electrospraying

Film material (particles size) [film thickness]	Substrate (process temperatures)	Solvent	Flow rate (deposition time or growth rate)	References
alumina (Al_2O_3) (100 nm)	aluminum (100–250°C substrate)	ethanol	0.8 ml/h or 1.5 ml/h (60 min)	[21]
gold (Au) (20, 30, 40, 60, 100 nm)	silicon (500°C annealing for 15 min)	water + stabilizer (citrate ligands)	6 μl/h (0.03 $\mu m^{-1}h^{-1}$ for 100 nm, 2 $\mu m^{-1}h^{-1}$ for 20 nm)	[35]
(20 nm)	silicon oxide // silicon	water (50 vol.%) + methanol (50 vol.%)	8 μl/h (6×10^7 particles/s) (horizontal spraying)	[13]
hydroxyapatite $Ca_5(PO_4)_3(OH)$ (50–80 nm)	glass	ethanol	6–10 ml/h	[48]
–	silicon (80°C substrate)	methanol	10 ml/h	[49]
–	glass	ethanol	60–420 μl/h	[51, 52]
(40 nm dia., 80 nm long)	glass or stainless steel	ethanol	60–180 μl/h	[16]
(40 nm dia., 80 nm long)	titanium or glass	ethanol	1.2 ml/h (60 s)	[15, 50]
molybdenite (MoS_2) (120×1000 nm – platelets) [280–1000 nm]	silicon	isopropanol, acetone, alcohol, or toluene	2.4 ml/h (25 min)	[40, 41]
nickel (Ni) (2–3 nm)	silicon (600°C annealing for 2 h in N_2)	ethylene glycol monoethyl ether acetate + alkylnaphthalene + polyamine		[39]
platinum (Pt) (5 nm) [0.3 mg/cm^2]	carbon (60°C substrate)	isopropanol + Nafion (33 wt.%)or [butylacetate (45%) + ethanol (50%) + glycerol (5%)] + Nafion (33 wt.%)	0.2–1 ml/h	[34]
PTFE (50–500 nm) [114 nm roughness]	FTO coated glass (150°C substrate; 265°C drying; 200°C curing in vacuum)	water + nonionic surfactant (6%)	0.6 ml/h (0.5–20 min)	[43, 44]
PZT (lead zirconate titanate)	Ti/Pt // silicon (75–175°C substrate, 650°C for 1200 s treatment)	1-propanol	90 μl/h (10–330 s)	[47]
silica (SiO_2) (20 nm)	quartz glass (600°C annealing for 2 h, ramp 5°C/min)	ethylene glycol	36 ml/h	[22, 24]
(10–30 nm)	silicon oxide // silicon	water (50 vol.%) + methanol (50 vol.%)	8 μl/h (6×10^7 particles/s) (horizontal spraying)	[13]
(5 nm)	glass slide	ethylene glycol	22 ml/h	[23]
silicon (Si) (3 nm)		1-octanol	0.1 μl/h	[14]
silver (Ag) (3–7 nm) [300–5000 nm]	polyimide	toluene	30 μl/h	[36]
(10 nm)	polyethylene terephthalate (200°C curing for 1 h)	water + polyvinyl alcohol	0.6 ml/h	[38]
(20 nm) [100–300 nm]	polyimide	ethylene glycol + surfactant	0.12 ml/h	[37]
zirconia (ZrO_2) (410 nm)	(1450°C sintering)	ethanol + 0.5% dispersant	3.3 ml/h (2 h)	[53]
(410 nm)	(1500°C sintering)	ethanol + 0.5% dispersant	0.36 ml/h (153 s for 100 layers)	[32]
(200 nm) [<10000 nm]	silicone release paper	butyl acetate (60 vol.%) + ethanol (40 vol.%)	0.6-45 ml/h (0.2 g/h)	[25]
zirconia + alumina composite (Al_2O_3+ZrO_2) (500 nm (Al_2O_3), 400 nm (ZrO_2))	quartz glass (1200°C sintering)	glycerol (for alumina), olive oil (for zirconia) + 1 wt.% dispersant	0.25–250 ml/h	[42]
zirconia + silicon carbide bi-layer (ZrO_2+SiC) (470 nm – ZrO_2, 1000 nm – SiC) [<10000 nm]	silicon or CrFe alloy	ethanol (50 vol.%) + water (50 vol.%)	0.4–1.8 ml/h (2 min)	[29]
zirconia stabilized with yttria (YSZ) (100 nm) [<2000 nm]	silicon coated with Pt (400°C substrate; 800°C sintering for 1 h, ramp: 3°C/min – heating, 2°C/min – cooling)	ethanol (50 vol.%) + acetylacetone (50 vol.%)	1–2 ml/h (0.5–1 h)	[33]

5. Conclusions

The paper provides experimental results of electrospray deposition of thin metal-oxide layer onto stainless steel substrate. The layer was produced from colloidal suspension of the material to be deposited in methanol. It has been demonstrated that metal oxide layers of various morphologies can be produced by this method. The layer morphology depends on the suspended material, the deposition rate, and the substrate temperature.

It can be concluded that electrospraying is a versatile tool for liquid atomisation, which has an advantage of uniform droplets generation for layer deposition purposes. Such layer-deposition system can operate at atmospheric conditions, and low or slightly elevated temperature. The electrospray operation at atmospheric conditions has an advantage of uniform micro- and nanothin film deposition on large areas without a special need for expensive installations. The electrospraying is a single-step, low-energy, and low-cost material processing technology, which can deliver the products of unique properties, with easily controlled deposition rate and film thickness via liquid flow rate and voltage to the capillary nozzle.

Acknowledgements. The paper is supported by Polish Ministry of Science and Higher Education within the Project No. 4078/T02/2007/32.

REFERENCES

[1] M. Cloupeau and B. Prunet-Foch, "Electrostatic spraying of liquids in cone - jet mode", *J. Electrostatics* 22, 135–159 (1989).

[2] M. Cloupeau and B. Prunet-Foch, "Electrostatic spraying of liquids. Main functioning modes", *J. Electrostatics* 25, 165–184 (1990).

[3] M. Cloupeau and B. Prunet-Foch, "Electrohydrodynamic spraying functioning modes. A critical review", *J. Aerosol Sci.* 25 (6), 1121–1136 (1994).

[4] J.M. Grace and J.C.M. Marijnissen, "A review of liquid atomization by electrical means", *J. Aerosol Sci.* 25 (6), 1005–1019 (1994).

[5] I. Hayati, A.I. Bailey, and Th.F. Tadros, "Investigations into the Mechanisms of Electrohydrodynamic Spraying of Liquids. Pt.I. Effect of electric field and the environment on pendant drop and factors affecting the formation of stable jets and atomization", *J. Coll. Interface Sci.* 117 (1), 205–221 (1987).

[6] I. Hayati, A.I. Bailey, and Th.F. Tadros, "Investigations into the Mechanisms of Electrohydrodynamic Spraying of Liquids. Pt.II. Mechanism of stable jet formation and electrical forces acting on a liquid cone", *J. Coll. Interface Sci.* 117 (1), 222–230 (1987).

[7] A. Jaworek and A. Krupa, "Classification of the modes of EHD spraying", *J. Aerosol Sci.* 30 (7), 873–893 (1999).

[8] A. Jaworek and A. Krupa, "Jet and drop formation in electrohydrodynamic spraying of liquids. A systematic approach", *Exp. Fluids* 27 (1), 43–52 (1999).

[9] I. Marginean, L. Parvin, L. Heffernan, and A. Vertes, "Flexing the electrified meniscus: The birth of a jet in electrosprays", *Anal. Chem.* 76, 4202–4207 (2004).

[10] I. Marginean, R.T. Kelly, J.S. Page, K. Tang, and R.D. Smith, "Electrospray characteristic curves: In pursuit of improved performance in the nanoflow regime", *Anal. Chem.* 79 (21), 8030–8036 (2007).

[11] I. Marginean, P. Nemes, and A. Vertes, "Astable regime in electrosprays", *Phys. Rev. E* 76 (2), paper no. 026320 (2007).

[12] D.Z. Wang, S.N. Jayasinghe, and M.J. Edirisinghe, "High resolution print-patterning of a nano-suspension", *J. Nanoparticle Res.* 7, 301–306 (2005).

[13] I.W. Lenggoro, H.M. Lee, and K. Okuyama, "Nanoparticle assembly on patterned "plus/minus" surfaces from electrospray of colloidal dispersion", *J. Coll. Interface Sci.* 303, 124–130 (2006).

[14] J.-U. Park, M. Hardy, S.J. Kang, K. Barton, K. Adair, D.K. Mukhopadhyay, Ch.Y. Lee, M.S. Strano, A.G. Alleyne, J.G. Georgiadis, P.M. Ferreira, and J.A. Rogers, "High-resolution electrohydrodynamic jet printing", *Nat. Materials* 6 (10), 782–789 (2007).

[15] X. Li, J. Huang, and M.J. Edirisinghe, "Novel patterning of nano-bioceramics: template-assisted electrohydrodynamic atomization spraying", *J. R. Soc. Interface* 5, 253–257 (2008).

[16] Z. Ahmad, E.S. Thian, J. Huang, M. J. Edirisinghe, S.M. Best, S.N. Jayasinghe, W. Bonfield, R.A. Brooks, and N. Rushton, "Deposition of nano-hydroxyapatite particles utilising direct and transitional electrohydrodynamic processes", *J. Mater. Sci.: Mater. Med.* 19, 3093–3104 (2008).

[17] M.V. Gopalakrishnan, K. Metzgar, D. Rosetta, and R. Krishnamurthy, "Structural characterisation and strength evaluation of spray formed ceramic composite near-net shapes", *J. Mater. Proc. Technol.* 135, 228–234 (2003).

[18] S.K. Chaudhury, C.S. Sivaramakrishnan, and S.C. Panigrahi, "A new spray forming technique for the preparation of aluminium rutile (TiO_2) ex situ particle composite", *J. Mater. Proc. Technol.* 145, 385–390 (2004).

[19] A. Jaworek, "Electrospray droplet sources for thin film deposition. A review", *J. Mater. Sci.* 42, (1), 266–297 (2007).

[20] A. Jaworek and A.T. Sobczyk, "Electrospraying route to nanotechnology: An overview", *J. Electrostatics* 66 (3–4), 197–219 (2008).

[21] C.H. Chen, M.H.J. Emond, E.M. Kelder, B. Meester, and J. Schoonman, "Electrostatic sol-spray deposition of nanostructured ceramic thin films", *J. Aerosol Sci.* 30 (7), 959–967 (1999).

[22] S.N. Jayasinghe, M.J. Edirisinghe, and D.Z. Wang, "Controlled deposition of nanoparticle clusters by electrohydrodynamic atomization", *Nanotechn.* 15, 1519–1523 (2004).

[23] S.N. Jayasinghe, "Self-assembled nanostructures via electrospraying", *Physica E* 33, 398–406 (2006).

[24] D.Z. Wang, S.N. Jayasinghe, M.J. Edirisinghe, and Z.B. Luklinska, "Coaxial electrohydrodynamic direct writing of nanosuspensions", *J. Nanoparticle Res.* 9, 825–831 (2007).

[25] W.D. Teng, Z.A. Huneiti, W. Machowski, J.R.G. Evans, M.J. Edirisinghe, and W. Balachandran, "Towards particle-by-particle deposition of ceramics using electrostatic atomization", *J. Mater. Sci. Lett.* 16, 1017–1019 (1997).

[26] C.H. Chen, E.M. Kelder, and J. Schoonman, "Effects of additives in electrospraying for materials preparation", *J. Europ. Ceramic Soc.* 18, 1439–1443 (1998).

[27] T. Nguyen and E. Djurado, "Deposition and characterization of nanocrystalline tetragonal zirconia films using electrostatic spray deposition", *Solid State Ionics* 138, 191–197 (2001).

[28] W. Balachandran, P. Miao, and P. Xiao, "Electrospray of fine droplets of ceramic suspensions for thin film preparation", *J. Electrostatics* 50 (4), 249–263 (2001).

[29] P. Miao, W. Balachandran, and P. Xiao, "Characterization of ZrO_2 and SiC ceramic thin films prepared by electrostatic atomization", *J. Mater. Sci.* 36, 2925–2930 (2001).

[30] P. Miao, W. Balachandran, and P. Xiao, "Formation of ceramic thin films using electrospray in cone-jet mode", *IEEE Trans. Ind. Appl*. 38 (1), 50–56 (2002).

[31] P. Miao, Z.A. Huneiti, W. Machowski, W. Balachandran, P. Xiao, and J.R.G. Evans, "Electrostatic atomization of ultra fine spray of ceramic solution", *Electrostatics 1999, Inst. Phys. Conf. Ser.* 163, 119–122 (1999).

[32] D.Z. Wang, M.J. Edirisinghe, and S.N. Jayasinghe, "Solid freeform fabrication of thin-walled ceramic structures using an electrohydrodynamic jet", *J. Am. Ceram. Soc.* 89 (5), 1727–1729 (2006).

[33] Z.Ch. Wang and K.-B. Kim, "Fabrication of YSZ thin films from suspension by electrostatic spray deposition", *Materials Letters* 62, 425–428 (2008).

[34] A.M. Chaparro, R. Benitez, L. Gubler, G.G. Scherer, and L. Daza, "Study of membrane electrode assemblies for PEM-FC, with cathodes prepared by the electrospray method", *J. Power Sources* 169, 77–84 (2007).

[35] P.H.M. Böttger, Z. Bi, D. Adolph, K.A. Dick, L.S. Karlsson, M.N.A. Karlsson, B.A. Wacaser, and K. Deppert, "Electrospraying of colloidal nanoparticles for seeding of nanostructure growth", *Nanotechn.* 18, paper no. 105304 (2007).

[36] K.J. Lee, B.H. Jun, T.H. Kim, and J. Joung, "Direct synthesis and inkjetting of silver nanocrystals toward printed electronics", *Nanotechn.* 17, 2424–2428 (2006).

[37] D.Y. Lee, Y.S. Shin, S.E. Park, T.U. Yu, and J. Hwang, "Electrohydrodynamic printing of silver nanoparticles by using a focused nanocolloid jet", *Appl. Phys. Lett.* 90, paper no. 081905 (2007).

[38] J.H. Yu, S.Y. Kim, and J. Hwang, "Effect of viscosity of silver nanoparticle suspension on conductive line patterned by electrohydrodynamic jet printing", *Appl. Phys. A* 89, 157–159 (2007).

[39] Y. Ishida, G. Nakagawa, and T. Asano, "Inkjet printing of nickel nanosized particles for metal-induced crystallization of amorphous silicon", *Japanese J. Appl. Phys.* 46 (9B), 6437–6443 (2007).

[40] J. Sobota and G. Sorensen, "Ion bombardment of MoS_2 nanoplatelet coatings deposited by electrospraying", *Tribology Lett.* 3, 161–164 (1997).

[41] G. Sorensen, "Ion bombardment of electrosprayed coatings: an alternative to reactive sputtering?", *Surf. Coat. Techn.* 112 (1–3), 221–225 (1999).

[42] K. Balasubramanian, S.N. Jayasinghe, and M.J. Edirisinghe, "Coaxial electrohydrodynamic atomization of ceramic suspensions", *Int. J. Appl. Ceram. Technol.* 3 (1), 55–60 (2006).

[43] E. Burkarter, C.K. Saul, F. Thomazi, N.C. Cruz, L.S. Roman, and W.H. Schreiner, "Superhydrophobic electrosprayed PTFE", *Surf. Coatings Techn.* 202, 194–198 (2007).

[44] E. Burkarter, C.K. Saul, F. Thomazi, N.C. Cruz, S.M. Zanata, L.S. Roman, and W.H. Schreiner, "Electrosprayed superhydrophobic PTFE: a non-contaminating surface", *J. Phys. D: Appl. Phys.* 40, 7778–7781 (2007).

[45] J. Lu, J. Chu, W. Huang, and Z. Ping, "Microstructure and electrical properties of Pb(Zr, Ti)O_3 thick film prepared by electrostatic spray deposition", *Sensors Actuators A* 108, 2–6 (2003).

[46] T. Wang and B. Derby, "Ink-jet printing and sintering of PZT", *J. Am. Ceram. Soc.* 88 (8), 2053–2058 (2005).

[47] D. Sun, S.S. Rocks, D. Wang, M.J Edirisinghe, and R.A. Dorey, "Novel forming of columnar lead zirconate titanate structures", *J. European Ceramic Soc.* 28, 3131–3139 (2008).

[48] J. Huang, S.N. Jayasinghe, S.M. Best, M.J. Edirisinghe, R.A. Brooks, and W. Bonfield, "Electrospraying of a nanohydroxyapatite suspension", *J. Materials Sci.* 39, 1029–1032 (2004).

[49] B.H. Kim, J.H. Jeong, Y.S. Jeon, K.O. Jeon, and K.S. Hwang, "Hydroxyapatite layers prepared by sol-gel assisted electrostatic spray deposition", *Ceramics Int.* 33, 119–122 (2007).

[50] X. Li, J. Huang, and M. Edirisinghe, "Development of nano-hydroxyapatite coating by electrohydrodynamic atomization spraying", *J. Mater. Sci.: Mater. Med.* 19, 1545–1551 (2008).

[51] E.S. Thian, Z. Ahmad, J. Huang, M.J. Edirisinghe, S.N. Jayasinghe, D.C. Ireland, R.A. Brooks, N. Rushton, W. Bonfield, and S.M. Best, "The role of electrosprayed apatite nanocrystals in guiding osteoblast behaviour", *Biomaterials* 29, 1833–1843 (2008).

[52] E.S. Thian, J. Huang, Z Ahmad., M.J. Edirisinghe, S.N. Jayasinghe, D.C. Ireland, R.A. Brooks, N. Rushton, S.M. Best, and W. Bonfield, "Influence of nanohydroxyapatite patterns deposited by electrohydrodynamic spraying on osteoblast response", *J.Biomed. Mater. Res. Part A,* 85A (1), 188–194 (2007).

[53] Q.Z. Chen, A.R. Boccaccini, H.B. Zhang, D.Z. Wang, and M.J. Edirisinghe, "Improved mechanical reliability of bone tissue engineering (zirconia) scaffolds by electrospraying", *J. Am. Ceram. Soc.* 89 (5), 1534–1539 (2006).